Photovoltaic Solar Application Study of $Cu_{0.5}Zn_{0.5}Se$ Thin Films by Chemical Bath Deposition Method

Kisan C. Rathod[a]* , Kallappa R. Sanadi[b], Pradip D. Kamble[c], Ganesh S. Kamble[d],

Muddsar L. Gaur[e], Kalyanrao M. Garadkar[f]

[a]The New College, Department of Chemistry, Kolhapur, MH, 416 012, India.
[b]Doodhsakhar Mahavidyalaya, Department of Chemistry, Bidri, Kolhapur, MH,416208, India.
[c]The New College, Department of Physics, Kolhapur, MH,416012, India.
[d]Kolhapur Institute of Technology's College of Engineering, Department of Engineering Chemistry, Kolhapur, (MH), 416234, India.
[e]C.B.Khedgi's Basaveshwar Science Raja Vijaysinh Commerce and Raja Jaysinh Arts College, Department of Chemistry, Akkalkot Solapur, MH,413216,India.
[f]Shivaji University, Department of Chemistry, Kolhapur, MH,416004, India.

Inorganic ternary type materials are induced compound is worked as fundamental applications in transformation of the solar light energy into electrical energy. Copper zinc selenide thin films have been synthesized by chemical bath deposition method on to stainless steel plate. The configuration of fabricated cell is p-$Cu_{0.5}Zn_{0.5}Se$| NaOH(1M) + S(1M) + Na_2S(1M) |$C_{(graphite)}$. The Photovoltaic cell characterization of the films is carried out by studying current–voltage characteristics in dark, capacitance–voltage in dark, barrier height measurements, power output, photoresponse and spectral response. The study shows that $Cu_{0.5}Zn_{0.5}Se$ thin films are p-type conductivity. The junction ideality factor was found to be 2.93. The flat band potential was found to be -0.708V. The barrier height value was found to be 0.186 eV. The study of power output characteristic shows open circuit voltage, short circuit current, fill factor and efficiency were found to be 150 mV, 21 µA, 42.13%, and 0.63%, respectively. Photoresponse shows lighted ideality factor is 2.89. Spectral response shows the maximum current observed at 580 nm.

Keywords: *CBD, Power output, Photo response, Flat band potential, Spectral response.*

1. Introduction

Due to the energy crises in the world and increasing demand of energy it is the need of our situation to develop new type of solar energy sources[1]. Conversion devices which have high power and energy density, which could the alternative source in the form of renewable energy[2]. In the world's energy demand is continuously increasing due to the rapid increase in population and decreasing in the natural sources, which is in the form of fossil fuels[3]. Copper zinc selenide is a narrow band gap material at room temperature. It is efficiently used in black, and red-light emitting diodes, photovoltaics, laser screens, thin film transistor and Photovoltaic cells[4-7]. In Photovoltaic cells (PVC), the interface which forms on mere dipping the semiconductor into electrolyte solution and the liquid junction potential barrier can be easily established. Polycrystalline semiconductor films can also be used without any drastic decrease in efficiency[8]. This is probably due to the intimate and perfect contact of liquid electrolyte with the crystalline grains. Thus, PVC cells provide an economic chemical route for trapping solar energy[9]. Along with PVC the semiconductor electrolyte -interface may be used for photoelectrolysis, photocatalysis and Photovoltaic power generation[10]. The properties of such systems are mainly dependent on the interface formed between the semiconductor electrode and electrolyte. Hence from material point of view, the microstructure of the photoelectrode surface is of main importance[11]. The advantage of PVC cells is simpler to make as compared to the p–n junctions which require highly pure semiconducting material[12,13]. Ternary chalcogenide is combined by utilizing different strategies. While $Mo(S_1-xSex)_2$ have been accounted for by utilizing arrested precipitation technique (APT), $CdIn_2Se_4$, $CuInS_2$ by Spray Pyrolysis[14,15], $Cu(InGa)Se_2$ thin films fabricated by means of single-target sputtering method[16] and InAlAs:Sb by metal-organic vapor phase epitaxy[17].

We report here the successful deposition of crystalline copper zinc selenide thin films by chemical bath deposition technique. Growth mechanism, structural, morphological, compositional, optical, electrical and thermoelectrical properties are studied[5]. This paper is devoted to Photovoltaic performance of chemically deposited $Cu_{0.5}Zn_{0.5}Se$ photo electrode. I–V, C–V characteristics, barrier height measurements, power out curves, photoresponse, and spectral response parameters are studied.

*e-mail: kishanchandurathod@gmail.com

2. Experimental Details

2.1. Construction and working of solar cell

A solar cell is a device that directly converts the energy of light into electricity energy through the photovoltaic effect is shown in Figure 1. Solar cells or photovoltaic cells are made based on the principle of the photovoltaic effect. They convert sunlight into direct current electricity. But single photovoltaic cell does produce enough amount of electricity. A solar cell is basically a junction diode although its construction it is little bit different from conventional p-n junction didoes is shown in Figure 2. A very thin layer of p-type semiconductor is grown on a one side and another side grown on a thick layer of the n-type semiconductor. Then apply a few finer electrodes on the top of the p-type semiconductor layer. These electrodes do not obstruct light to reach the thin p-type layer there is a p-n junction. Then we also provide a current collecting electrode at the bottom of the n-type layer. As the concentration of electrons becomes higher in n-type side of the junction and concentration of holes becomes more in another p-type side. A voltage is set up which is known as photo voltage and it connect a small load across the junction and there will be a tiny current flowing through it.
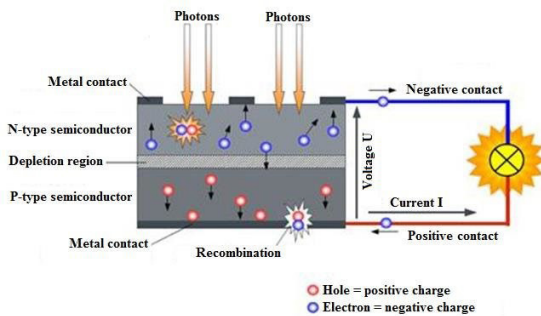

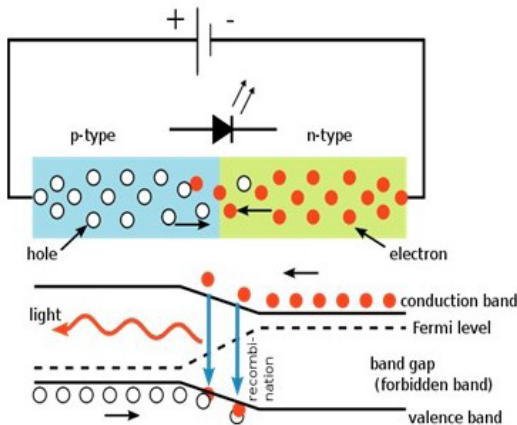**Figure 1.** Construction and working of solar cell.

Figure 2. Formation of the p-n junction diode in the solar cell.

2.2. Preparation of $Cu_{0.5}Zn_{0.5}Se$ photovoltaic electrode

All the chemicals used for the deposition were analytical grade. It includes copper sulphate pentahydrate, zinc sulphate, tartaric acid, liquor ammonia, sodium sulfite and selenium powder. All the solutions were prepared in double distilled water. Sodium selenosulphate was prepared by the following the method reported earlier[18,19]. The deposition of $Cu_{0.5}Zn_{0.5}Se$ thin films were made from a reactive solution obtained by mixing 5mL (0.2M) copper sulphate, 5 mL (0.2M) zinc sulphate, 2.5 mL (1M) tartaric acid, and 10 mL (0.25M) sodium selenosulphate and finally diluted to 80 mL by adding double distilled water. The beaker containing the reactive solution was kept at room temperature. The pH of the resulting solution was found to be 10 ±0.05. Four cleaned stainless-steel substrates were positioned vertically on a specially designed substrate holder and rotated in a reactive solution with a speed of 60±2 rpm. Figure 3. is shown in the experimental setup of the thin film deposition. The temperature of the solution was then allowed to rise slowly to 300 K. After seven hours, the stainless-steel substrates were removed, washed several times with double distilled water, dried naturally preserved in dark desiccators over anhydrous $CaCl_2$. The resultant films were homogenous, well adherent to stainless steel substrate.

2.3. Fabrication of Photovoltaic cell

Photovoltaic cell consisting in three electrode configurations are used in this experiment. $Cu_{0.5}Zn_{0.5}Se$ as photo anode, CoS-treated graphite rod as a counter electrode. This electrode acts as a photocathode. A calomel electrode was used as reference electrode and sulphide–polysulphide as electrolyte is shown in Figure 4.

2.4. Characterization of PVC cell

The type of conductivity exhibited by the film is determined by nothing the polarity of the emf developed in PVC cell under illumination. The illuminated area of electrode was 3.0 cm^2.
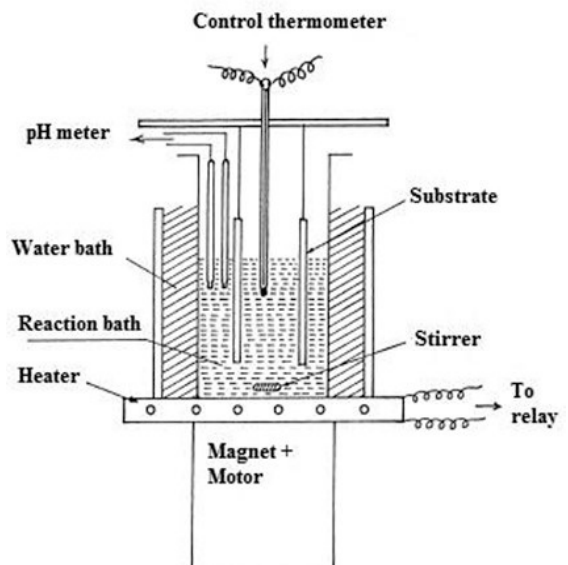

Figure 3. Experimental setup of CBD method deposition of thin film.

The Mott–Schottky plot is used to determine the flat band potential One-kilohertz frequency is used to determine the flat band potential. The current–voltage (I–V) characteristic in dark has been plotted. The junction ideality factor has been determined by plotting the graph of log I versus V. The fill factor and power conversion efficiency of the cell is calculated from photovoltaic power output characteristics. The power output characteristic has been obtained for a PVC cell at a constant illumination of 30 mW/cm^2. The barrier height was examined from temperature dependence of reverse saturation current at different temperature. Light ideality factor was measured from photoresponse. Spectral response was determined by measuring short circuit current as well as open circuit voltage as function of incident light.

3. Results and Discussion

3.1. Conductivity type

A photovoltaic cell with configuration p- Cu$_{0.5}$Zn$_{0.5}$Se | NaOH (1M) + S (1M) + Na$_2$S (1M) | C$_{(graphite)}$ was formed. Photovoltaic cell shows dark voltage and dark current even in the dark. The polarity of this dark voltage was negative towards semiconductor electrode. The sign of the photovoltage gives the conductivity type of Cu$_{0.5}$Zn$_{0.5}$Se. This suggests that Cu$_{0.5}$Zn$_{0.5}$Se is an p-type conductor which has also been proved from TEP measurement studies[5,20].

3.2. I–V characteristics in dark

Current–voltage (I–V) characteristics of Photovoltaic cell in dark have been studied at 305 K and shown in Figure 5 show I-V curves for the films with composition of Cu/Zn = 0.5. The characteristics are non-symmetrical indicating the formation of rectifying type junction[21]. Using
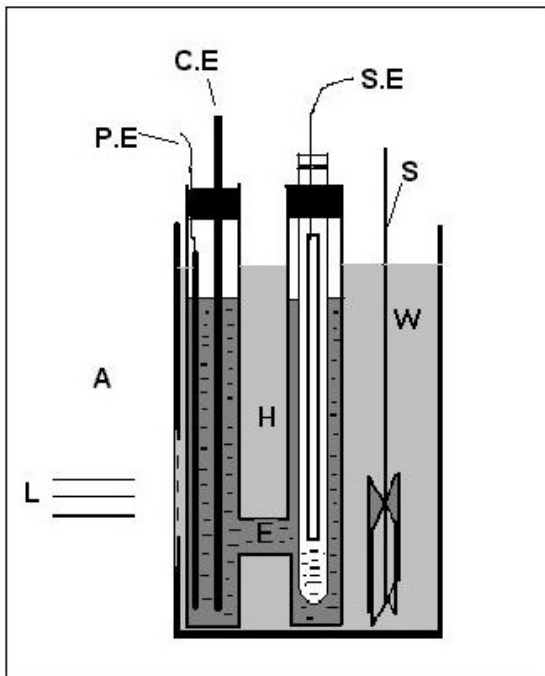
famous ideal Schottky diode equation junction ideality factor is calculated from the equation[22,23].

$$I = \left[\left(I_0 e^{ev} \right) / \left(n_d kT \right) \right] \qquad (1)$$

Where, I, is the forward current in dark, I$_0$, reverse saturation current, v, applied forward bias voltage and n$_d$ is the junction ideality factor. The value of junction ideality factor (nd) can be determined of the linear regions of the log I versus volt (V) are shown in Figure 6. Slop of the variation is divided by the 16.8736 then junction ideality factor was found to be 2.93. The n$_d$ values were found to be higher than the ideal value, a common fact found in many polycrystalline photoelectrode materials and is indication of the fact that the current transport across the interface has the influence of other kinds of recombination mechanisms and series resistance effect the former is due to the presence of the surface states[24,25].

3.3. C–V characteristics in dark

The measurements of capacitance as a function of applied voltage provided useful information such as type of conductivity, depletion layer width and flat band potential
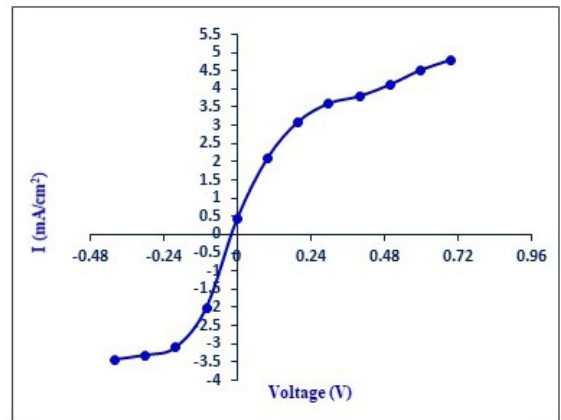

Figure 5. I–V characteristics of Cu$_{0.5}$Zn$_{0.5}$Se photoelectrode (in dark).

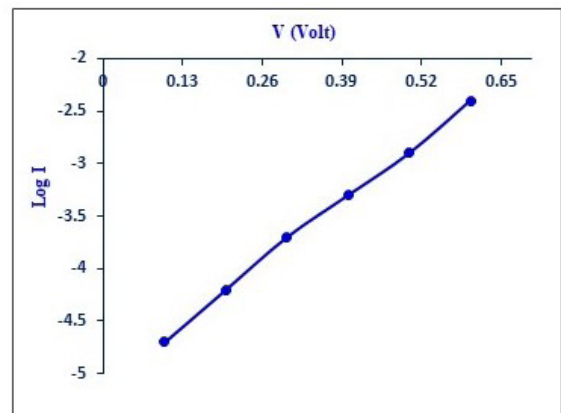**Figure 6.** Determination of junction ideality factor of Cu$_{0.5}$Zn$_{0.5}$Se photoelectrode.

Figure 4. A Schematic diagram of photovoltaic solar cell electrode.

(V_{fb}). The flat band potential of a semiconductor gives information of the relative position of the Fermi levels in photoelectrode as well as the influence of electrolyte and charge transfer process across the junction. This is also useful to measure the maximum open circuit voltage (V_{oc}) that can be obtained from a cell. Measured capacitance is the sum of the capacitance due to depletion layers and Helmholtz layer in electrolyte which is neglected by assuming high ionic concentration[26]. Under such circumstances, V_{fb} can be obtained using Mott–Schottky relation by standardizing with saturated calomel electrode.

$$C^{-2} = \left[2 / \left(q \varepsilon_s \varepsilon_0 \, N_d \right) \right] \times \left[\left(V - V_{fb} - kT \right) / q \right] \quad (2)$$

Where the terms involved have meaning, C^{-2} is space charge capacitance per unit area, q the electronic charge, ε_s is the dielectric constant of the semiconductor electrode, ε_0 is the permittivity of the free space, N_d the donor density, k the Boltzmann constant, T the absolute temperature, V the applied potential and V_{fb} is the flat band potential. The $1/C^{-2}$ against voltage (V) (Mott-Schottky plot) were constructed for the sample and are shown in Figure 7. It is observed that the flat band potential become more positive versus SCE as Zn^{2+} concentration in the electrode ratio of Cu/Zn = 0.5 there after it saturates and diminishes. This fact may be correlated to the decrease in the electron affinity as a result of introduction of Zn^{2+} ions in the lattice of CuSe an increased amount of surface adsorption and creation of new acceptor levels. All these effects are responsible for band bending observed in the semiconductor electrode. The nature of plot suggests the presence of two regions corresponding to shallow and deep donor levels[27]. Intercepts of plots on voltage axis determine the flat band potential value. The flat band potential value found to be -0.708 V for $Cu_{0.5}Zn_{0.5}$Se –polysulphide redox electrolyte, which is a measure of electrode potential at which band bending is zero. The non-linear nature of the graph is an indication of graded junction formation between $Cu_{0.5}Zn_{0.5}$Se and polysulphide electrolyte.

3.4. Barrier height measurements

The barrier height was determined by measuring the reverse saturation current (I_0) through the junction at different temperature from 323 to 303 K. The reverse saturation current flowing through junction is related to temperature as,[22,23,27]

$$I_0 = AT^2 \exp \left[\Phi_\beta / kT \right] \quad (3)$$

Where, A is Richardson constant, k the Boltzmann constant, Φ_β is the barrier height in eV. To the determination of the barrier height of the photoelectrode, a graph of log (I_0/T^2) with 1000/T was plotted. The plot of log (I_0/T^2) with 1000/T for representative sample is shown in Figure 8. The values of barrier height were determined from the linear regions of the plots. The observed nonlinearity of plots in high temperature regions can attributed to Pool-Frankel type of conduction mechanism[28]. From the slope of the linear region of plots, the barrier height was determined. The barrier height value is found to be 0.186 eV.
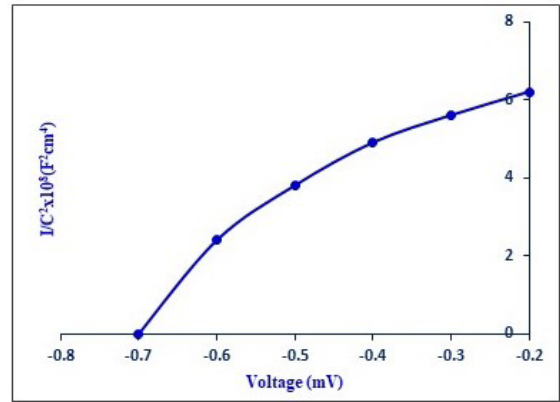

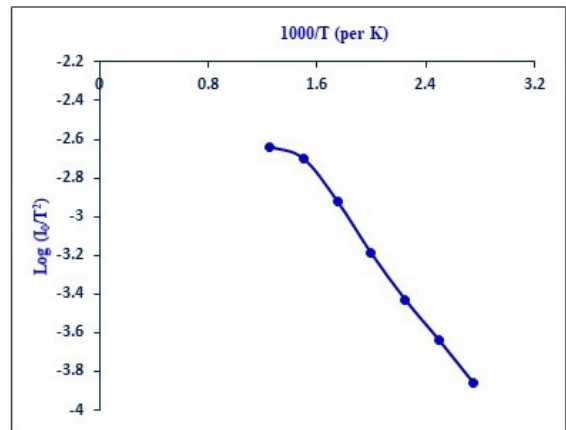**Figure 7.** C–V plots (Mott-Schottky plots) of $Cu_{0.5}Zn_{0.5}$Se photoelectrode.

Figure 8. Determination of barrier height measurement of $Cu_{0.5}Zn_{0.5}$Se photoelectrode.

3.5. Power output characteristics

When a photovoltaic solar cell is illuminated with the light constant intensity of the current voltage characteristics shift in the four quadrant this behavior is in accordance with the theory of solar cells acting as electricity generator. As the Photovoltaic cell may operate over a wide range of voltages and currents. By applying the resistive load on an irradiated cell continuously from a short circuit to a very high value of open circuit it is possible to determine the maximum power point ($P_m = V_m \times I_m$), that is the load for which the cell can deliver maximum electrical power. The Energy conversion efficiency (η 'eta') of a cell is the percentage of power converted of the observed light to electrical energy, and collected and are shown by the following equation.

$$\left[n = P_m / \left(E \times A_c \right) \right] \quad (4)$$

Where E is power of input light (mW/cm^{-2}) and A_c is the surface area of the cell in cm^2. Another measuring term in the overall behavior of a cell is the fill factor (ff), which is the ratio of the maximum power ($V_m \times I_m$) divided by the short circuit current (I_{sc}) and open circuit voltage (V_{oc}) in

light current voltage (I-V) characteristics of the cells can be measured by the following equation.

$$ff = \left[p_m / \left(V_{oc} \times I_{sc} \right) \right] = \left[\left(\eta \times E \times A_c \right) / \left(V_{oc} \times I_{sc} \right) \right] \qquad (5)$$

The photovoltaic power output characteristics for a cell under illumination of 30 mW/cm^2 shows Figure 9. The maximum power output of the cell is given by the largest rectangle that can be drawn inside the curve. The open circuit voltage and short circuit current are found to be 150 mV and 21 μA, respectively. The power efficiency conversion factor can be studied by the following equation.

$$\eta_{max} = \left[V_{redox} - V_{fb} \right] \times \left[e / E_g \right] \qquad (6)$$

Where V_{fb} is the flat band potential, V_{redox} the electrolyte redox potential and E_g is the energy band gap. It is important to note here that V_{oc} and η depends on V_{fb} and E_g. The magnitude of η and ff increases with the ratio of Cu/Zn is 0.5. The calculated fill factor is 42.13%. The power conversion efficiency is found to be 0.63%. The low efficiency may be due high series resistance and interface states which are responsible for recombination mechanism. The value of series resistance and shunt resistance are found to be 796 (Ω) and 500 (Ω), respectively. In this situation, the Photogenerated charge carriers can move in both the direction. Lee et.al.[29] reported that the photogenerated electrons for the cell with p-type photoanode, any increase in the value of V_{fb} corresponds to increase in the value of open circuit photo potential of the p-type material either recombine readily with holes into the electrolyte, instead of flowing through external circuit.

3.6. Photoresponse

The PVC cell towards light, the cell was illuminated with light of different intensity. The open circuit voltage and short circuit current were measured as function of light intensity. Figure 10 shows variation of shot circuit current (Isc) as a function of light intensity, whereas, Figure 11 shows the variation of open circuit voltage as a function of light intensity. The photoresponse measurements showed a logarithmic variation of open circuit voltage with the incident light intensity. However, at higher intensities,
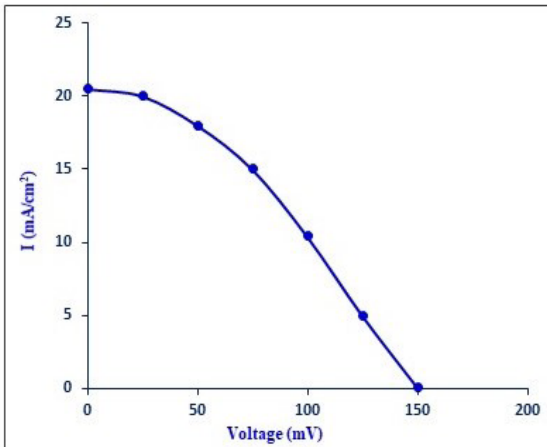
saturation in open circuit voltage was observed, which can be attributed to the saturation of the electrolyte interface, charge transfer and non-equilibrium distribution of electrons and holes in the space charge region of the photoelectrode. But short circuit current follows almost a straight-line path. The photoelectrode–electrolyte interface can be modeled as a Schottky barrier solar cell[30] and it is therefore possible to represent the current–voltage relationship as;

$$I = I_{ph} - I_d = I_{ph} - \left[I_0 \exp \left(qV / n_d kT \right) \right] - 1 \qquad (7)$$

Where I is the net current density, 'I_{ph}' the photocurrent densities, 'I_d'the dark current density, I_o the reverse saturation current density, V the applied bias voltage and n_d is the junction ideality factor. In bias voltage condition V>3kT/q and at equilibrium open circuit conditions.

$I_{ph} = I_d$ and $V = V_{oc}$ thus,

$$V_{oc} = \left[n_L kT / q \right] \times \ln \left[I_{sc} / I_0 \right] \qquad (8)$$

where V_{oc} is the open circuit voltage and I_{sc} is the short circuit current. As $I_{sc} \gg I_o$, a plot of log I_{sc} against V_{oc} should give a straight line and from the slope of the line the lighted ideality factor can be determined. The plot of log I_{sc} with V_{oc} for Cu$_{0.5}$Zn$_{0.5}$Se photo electrode is shown in Figure 12. The
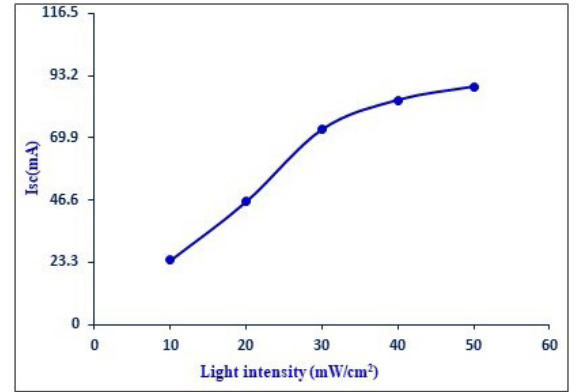

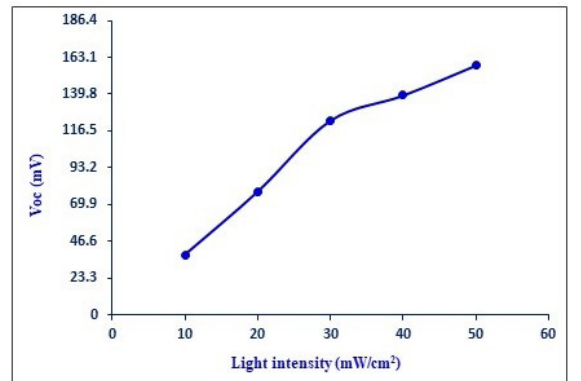**Figure 10.** Photo response as a function of short circuit current for Cu$_{0.5}$Zn$_{0.5}$Se photoelectrode.

Figure 9. Power output curves for Cu$_{0.5}$Zn$_{0.5}$Se photoelectrode.

Figure 11. Photo response as a function of open circuit voltage for Cu$_{0.5}$Zn$_{0.5}$Se photoelectrode.
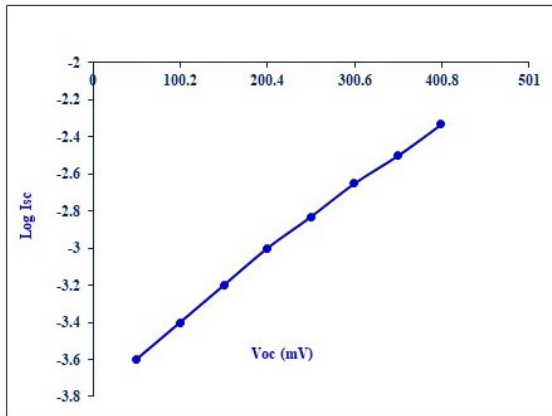
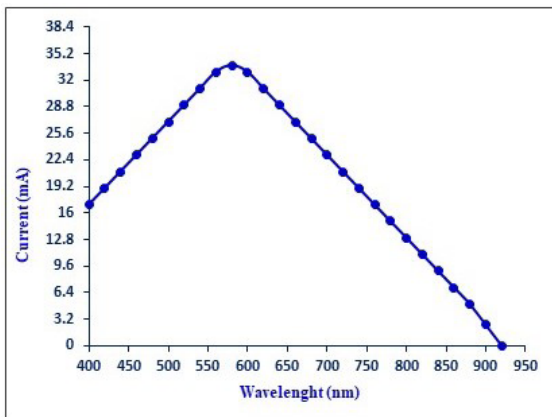**Figure 12.** Determination of lighted ideality factor for $Cu_{0.5}Zn_{0.5}Se$ photoelectrode.

Figure 13. Determination of spectral response for $Cu_{0.5}Zn_{0.5}Se$ photoelectrode.

slope of the variation is multiplied by 1.68523 and lighted ideality factor was found to be 2.89.

3.7. Spectral response

Photovoltaic cell is one of the most powerful techniques to measure the performance of the spectral response cell qualitatively. Therefore, the spectral response of a cell has been recorded in the 400–920 nm wavelength range. The photocurrent action spectra were examined and are shown in Figure 13. It is seen that spectra attain maximum value of current at λ = 580 nm and decreases with increase in wavelength. The decrease in current on longer wavelength side may be attributed to non-optimized thickness and transition between defect levels. The maximum current is obtained corresponding to λ = 580 nm gives band gap value 1.9 eV for agreeing with the results of optical absorption studies[5,10,19].

4. Conclusion

The Photovoltaic solar cells with the photoanode of the type $Cu_{0.5}Zn_{0.5}Se$ have been constructed and investigated for the cell properties as a function of photoelectrode composition Cu/Zn ratio 0.5. The results indicated that for the $Cu_{0.5}Zn_{0.5}Se$ efficiency and the fill factor were increased to 0.63% to 42.13% respectively. The observed enhancement due to increased open-circuit voltage, and improved photoelectrode absorption. The observed conversion efficiencies are found to be lower due to lack of post preparative treatments. The solar cell can be easily fabricated using $Cu_{0.5}Zn_{0.5}Se$ photo anode, sulphide–polysulphide as electrolyte, CoS-treated graphite rod as a counter electrode. A saturated calomel electrode was used a reference electrode. The various performance parameters were determined for $Cu_{0.5}Zn_{0.5}Se$ photo electrode.

5. Acknowledgments

6. References

1. Bhapkar UV, Mattauch RJ. Numerical simulation of the current-voltage characteristics of heteroepitaxial Schottky-barrier diodes. IEEE Trans Electron Devices. 1993;40(6):1038-1046.
2. Buch F, Fahrenbruch AL, Bube RH. Photovoltaic properties of five II–VI heterojunctions. J Appl Phys. 1977;48:1596-1602.
3. Bube RH, Buch F, Fahrenbruch AL, Ma YY, Mitchell W. Photovoltaic energy conversion with n-CdS-p-CdTe heterojunctions and other II–VI junctions. IEEE Trans Electron Devices. 1977;24(4):487-492.
4. Katagiri H, Sasaguchi N, Hando Oshino S, Ohashi J, Yokota T. Energy efficiency of photovoltaic cell based. Sol Energy Mater Sol Cells. 1997;49:407-14.
5. Rathod KC. Optical structural and morphological studies of Cu0.5Zn0.5Se thin film deposited by chemical bath deposition method. J. Material Today: Proceedings. 2020;23:260-6.
6. Tanaka T, Kawasaki D, Nishio M, Guo Q, Ogawa H. Fabrication of Cu2ZnSnS4 thin films by co-evaporation. Phys Status Solid C. 2006;3(8):2844-7.
7. Katagiri H, Sasaguchi N, Hando S, Hoshino S, Ohashi J, Yokota T. Preparation and evaluation of Cu2ZnSnS4 thin films by sulfurization of E–B evaporated precursors. In: 9th International Photovoltaic Science and Engineering Conference; Miyazaki. Proceedings. Miyazaki: International PVSEC-9; 1996. pp. 745-6.
8. Potlog T, Spalatu N, Fedorov V, Maticiuc N, Antoniuc C, Botnariuc V, et al. The performance of thin film solar cells employing photovoltaic ZnSe/CdTe, CdS/CdTe and ZnTe/CdTe heterojunctions. In: 37th IEEE Photovoltaic Specialists Conference (PVSC); 2011 June 19-24; Seattle. Proceedings. Seattle: Conference Record of the IEEE Photovoltaic Specialists Conference; 2011; pp. 1365-70.
9. Chandra S. Photoelectrochemical solar cells. London: Gordan and Breach; 1984.
10. Katagiri H, Saito K, Washio T, Shinohara H, Kurumadani T, Miyajima S. Development of thin film solar cell based on Cu2ZnSnS4 thin film. Sol Energy Mater Sol Cells. 2001;65:141-8.
11. Seol J, Lee S, Nam H, Kim K. Electrical and optical properties of Cu2ZnSnS4 thin films prepared by RF magnetron sputtering process. Sol Energy Mater Sol Cells. 2003;75:155-62.
12. Shashidhara A, Kasturi VB, Shivakumar GK. Electrical characterization of vacuum-deposited p-CdTe/n- ZnSe heterojunction. J Appl Nanosci. 2015;5:1003-7.
13. Christoper EH, Dennis JF, Andrew RB. Thin film CdSe/CuSe photovoltaic on a flexible single walled carbon nanotube substrate. Chem Chem Phys. 2013;15:3930-8.

14. Nikale VM, Suryavanshi UB, Bhosale CH. Effect of substrate temperature on spray deposited CdIn2Se4 thin films. Mater Sci Eng B. 2006;134:94.

15. Bhuse VM, Hankare PP, Sonandkar S. Structural, optical, electrical and photo-electrochemical studies on indium doped Cd0.6Hg0.4Se thin films. Mater Chem Phys. 2011;101(2-3):303-9.

16. Zhang S, Wu L, Yue R, Yan Z, Zhan H, Xiang Y. Effects of Sb-doping on the grain growth of Cu(In, Ga)Se2 thin films fabricated by means of single-target sputterin. Thin Solid Films. 2013;527:137.

17. Gaur ML, Bhuse VM, Sanadi KR. Antimony induced Cd0.4Co0.6Se thin films: Study of photovoltaic performance vy simple chemically grown method. Optik. 2021;227: 166057.

18. Pathan HM, Lokhande CD. Chemical deposition and characterization of copper indium diselenide (CISe) thin films. J Applied Surf Sci. 2005;245:328.

19. Hankare PP, Khomane AS, Chate PA, Rathod KC, Garadkar KM. Preparation of copper selenide thin films by simple chemical route at low temperature and their characterization. J Alloys Compd. 2009;469:478.

20. Mauk PH, Tavakolian H, Sites JR. Interpretation of thin-film polycrystalline solar cell capacitance. IEEE Trans Electron Dev. 1990;37(2):422-7. http://dx.doi.org/10.1109/16.46377.

21. Bhuse VM, Hankar PP, Garadkar KM, Khomane AS. A simple, convenient, low temperature route to grow polycrystalline copper selenide thin films. J Mater Chem Phys. 2003;80:82.

22. Lade SJ, Uplane MD, Lokhande CD. Growth and characterization of nanocrystalline CdSe thin films deposited by the successive ionic layer adsorption and reaction method. J Mater Chem Phys. 2001;68:36.

23. Deshmukh LP, Shahane GS. CdS-Se thin film electrodes: an electrochemical photovoltaic study. Int J Electron. 1997;83:341.

24. Gutierrez MT, Ortega J. Characterization and photoelectrochemical properties of chemical bath deposited n-PbS thin films. Sol Energy Mater. 1990;20:387.

25. Al AM, Al Dhafiri AAI. 8.6% Efficiency CZTSSe solar cell with atomic layer deposited Zn-Sn-O buffer layer. Sol Energy Mater Sol Cells. 1994;33:4865.

26. Le Meur MA, Cuniot M, Rommeluere JF, Tromson-Carli A, Triboulet R, Marfaing Y. Advances in HgCdTe N-P-N-P photoconductive structures. J Cryst Growth. 1998;184-185:1279-83. http://dx.doi.org/10.1016/S0022-0248(98)80265-0.

27. Lour WS, Chang CC. VPE grown ZnSeSi PIN-like visible photodiodes. Solid-State Electron. 1996;39:1295-8. http://dx.doi.org/10.1016/ 0038-1101(96)00033-0.

28. Spalatu N, Serban D, Potlog T. ZnSe films prepared by the close-spaced sublimation and their influence on ZnSe/CdTe solar cell performance. In: International Semiconductor Conference (CAS); 2011 Oct 17; Sinaia. Proceedings. Sinaia: CAS; 2011. pp. 445-54.

29. Lee Y, Gray J. Photovoltaic solar energy conference. In: 12th European Photovoltaic Solar Energy Conference; 1994 April 11-15; Amsterdam. Proceedings. Bedford: Stephens; 1994. pp. 1561-4.

30. McElhany P, Arch J. Numerical simulation of Cu2ZnSnS4 based solar cells with In2S3 buffer layers by SCAPS-1D. Appl Phys. 1988;64:1254.